

FEM Analyses and Experimental Study of Bearingless Motor with Rectifier Circuits

Li Chen, Hironobu Aratani, and Koichi Oka

Kochi University of Technology, Miyanokuchi 185, Tosayamada-cho, Kochi 782-8502, Japan

Abstract--In this paper, a feasibility study for a new type of bearingless motor is carried out by FEM analyses. The feature of the bearingless motor is using a rotor with rectifier circuit coils. The optimum geometrical dimensions of the proposed bearingless motor are determined by the rotor torques at various rotor tooth lengths. The dimensions are chosen by relatively minimum fluctuation and avoiding small torques. In order to generate the radial forces, a control currents arrangement is proposed. FEM analyses are also used for evaluating the property of the proposed arrangement. The results verify the feasibility of the proposed bearingless motor.

Index Terms: Bearingless motor, FEM analysis, Rectifier circuit coil, Radial force.

I. INTRODUCTION

Bearingless motor mechanism has functions of both a magnetic bearing and a motor. It is therefore able to suspend the rotor and generate torque simultaneously. Bearingless motor has not only the advantages of magnetic bearing such as negligible friction loss, no wear, high reliability, low-maintenance, higher speed for extreme environment, and no need of complex lubrication, but also has a shorter shaft compared with a shaft using both a conventional motor and a magnetic bearing. The critical rotating speed can be increased and its volume can be reduced. Bearingless motors can be used at some special fields such as artificial hearts, high speed drives, and generators. Since bearingless motors have so many advantages and special applications, various types of bearingless motors have been developed [1]-[2].

From a view of motor types, permanent magnet bearingless motors are widely developed. Permanent magnet bearingless motors are more effective even with a relatively large air gap. It is helpful to reduce the motor volume using permanent magnet. However, for permanent magnets, there are also some disadvantages, such as demagnetization and limited mechanical strength [3].

Another type of bearingless motor has been proposed [4]. The feature of the proposed motor is that there is a rectifier circuit in the rotor winding. The feasibility analysis had been carried out by means of simple numerical simulation. The proposed bearingless motor possesses such advantages as no demagnetization, much less rotor reluctance and being liable to realize serial production. In this paper, further study results are

presented, FEM analyses show that the proposed structure can be put into practice.

II. PRINCIPLE OF THE PROPOSED BEARINGLESS MOTOR

An illustration of a rectified bearingless motor is shown in Fig.1. It has a four poles rotor and eight poles stator. Details of one set of rotor, stator and coils are illustrated in Fig.2. In the figure, there are two sets of coils on the stator poles.

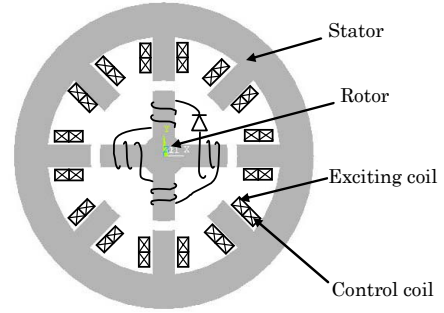


Fig. 1. Illustration of rectified bearingless motor

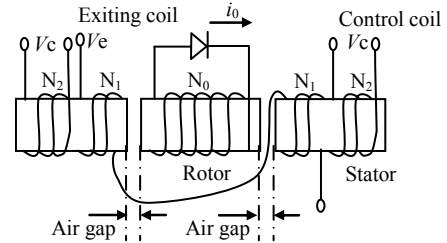


Fig. 2. Schematic of rectified rotor and stator

One set of coils are connected with the opposing stator coils in series. These coils are excited by AC current and called as exciting coils. Another set of coils are called as control coils, which are used to control the rotor torque and radial force.

In addition, one set of coils are wound on the rotor poles in series, and a rectifier diode is joined to the rotor winding circuit. When AC current is applied to the exciting coil, DC current will be induced in the rotor windings owing to the existence of the rectifier diode, therefore the rotor possesses fixed polarity poles.

Fig.3 shows the simulation results of exciting voltage, induced rotor current and rotor flux. It can be seen that when AC current is applied to the exciting coil, DC current is induced in the rotor coil, and the rotor flux almost keeps constant.

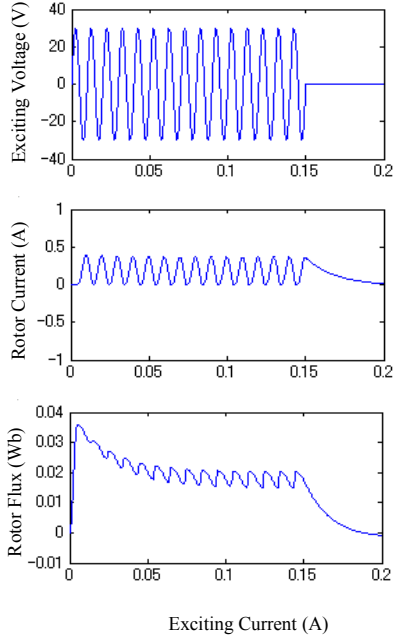


Fig. 3. Fuction of rectified circuit coil

Moreover, the rotor is made of silicon iron, the reluctance of which is much less than that of permanent magnet and the demagnetization will not take place. Adjusting the magnitude and directions of control current can control the radial force and the rotation torque, and the motor can work just like a noncontact PM stepping motor.

III. PROTOTYPE DESIGN AND ANALYSIS

A. Design of rectified bearingless motor

A prototype bearingless motor is designed as shown in Fig. 4. The radius of the rotor is determined to be 60 mm. It is decided by easiness of treatment. The shape of the

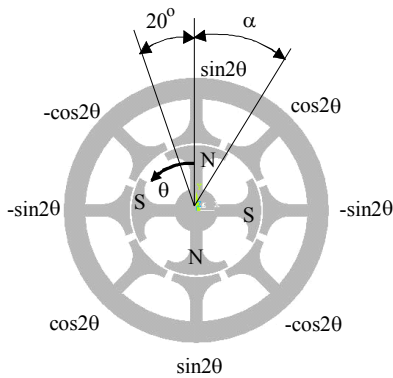


Fig. 4. Shape of rotor, stator and rotation strategy

stator or the rotor is like an unfolded fan because of the necessity of large area where the stator and the rotor face to each other. The induced current must be generated by mutual inductance which depends on the faced area. The angle of the stator tooth has 40 degrees which is twice to 20 degrees shown in Fig. 4. This value is determined by the consideration for the widest stator tooth. The required

angle for the gap to the next tooth is considered as at least 5 degrees. The angle of the rotor is indicated as α . The coils wound on the rotor and stator poles are identical to those shown in Fig.1.

Since the shape of rectified bearingless motor has been determined, an optimum dimension α of the bearingless motor is desired so that a relatively large radial force and torque can be generated. Based on the assumption that the rotor is located at the geometrical centre of the motor and it is magnetized by uniform induced current, a series of FEM analyses have been carried out to determine α .

In order to rotate the rotor, the sine and cosine control current arrangement about the rotation angle is applied as shown in Fig. 4. In the figure, α is the rotational angle of the rotor which rotates in counter clockwise. The rotor position in Fig. 4 indicates 0 degree. The torques at various angular positions have been calculated when α changes from 15 degrees to 40 degrees with the incremental angle being 5 degrees. These variations of α are corresponding to shorter, equal, and longer than the stator tooth length. Fig. 5 is an example of the flux distribution when α is 30 degrees. It can be seen that much more flux lines flow between the stator and the adjacent rotor tooth.

Because of the symmetrical configuration of the rotor and the stator, analyses of the rotor angle from 0 degree to 90 degrees have been examined. The results of torque are shown in Fig. 6. As shown in the figure, when the angle

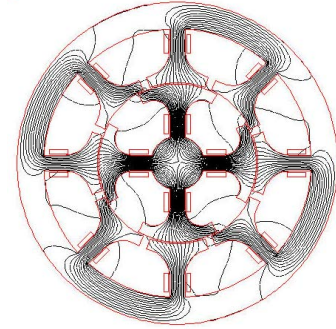


Fig. 5. Schematic of flux distribution at α of 30 degrees

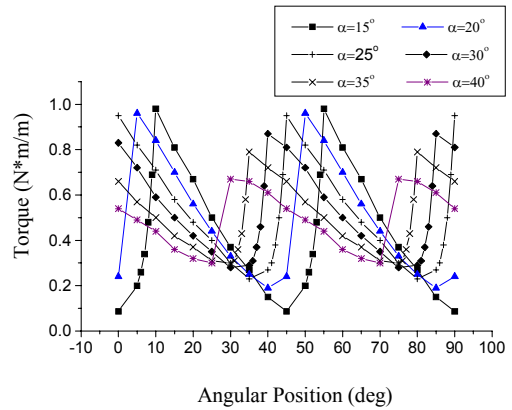


Fig. 6. Torques of various α vs. rotating angle

of the rotor tooth increases, the curve of the torque becomes flat. It can be found that a relatively large and

smooth torque can be obtained when α is equal to 30 degree. Thus, the 30 degrees of α has been chosen for the prototype bearingless motor. It can also be seen that the torque approaches its maximum when the rotor pole front edge begins to align with the stator tooth face at all α . For example, when α is equal to 15 degrees, and the rotor angle position α is 10 degrees, the torque reaches its maximum when the front edge of rotor pole begins to overlap with the next stator tooth face.

B. Control current arrangement for radial force

In order to verify the validity of the control current arrangement for the radial force control, a series of FEM analyses have been carried out. The control current arrangement is determined as shown in Fig. 7. This arrangement is for the vertical direction (y direction). The radial forces and torque have been calculated at various rotor angular positions.

The results are shown in Fig. 8 and Fig. 9. From Fig. 8, it can be seen that the radial forces are about ten times to the lateral forces. As a result, the radial forces can be guaranteed by the control current arrangements shown in Fig. 7. Fig. 9 shows the torques when we applied the currents of the radial force. Torques are negligible

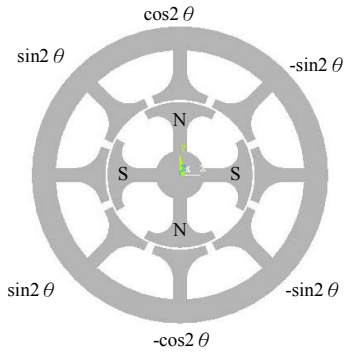


Fig. 7. Control current arrangement for vertical force

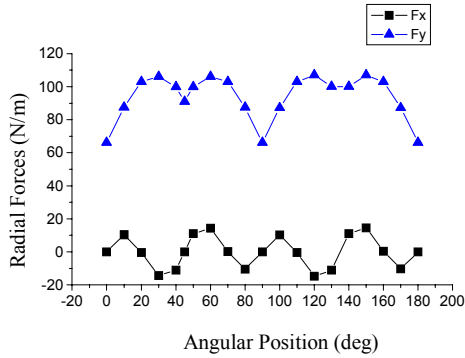


Fig. 8. Radial forces vs. rotor angular positions

compared with those shown in Fig. 6. For horizontal force, the corresponding current arrangement can be applied.

The superposition of the control current arrangements illustrated in Fig. 4 and Fig. 7 can be used to realize rotor rotation and vertical radial force control, meanwhile the superposition of the control current arrangements of the torques and horizontal force can be used to control the rotor rotation and horizontal radial force.

C. Linearity of input current and radial force

For levitation of a bearingless motor, constant suspension forces are desired, nevertheless the radial forces fluctuate with the rotor angular positions as shown in Fig. 8. This problem may be reduced by feedback control. Since feedback control is easy to be applied for a linear system, the linearity of input current and output force has been examined. The linearity is examined by changing an amplitude constant k which is a multiplying coefficient to control currents. For the control current arrangement of the vertical direction forces shown in Fig. 7, as changing the constant k from 0 to 1 with the incremental value being 0.2, the radial forces in the vertical direction have been calculated.

The results of the forces with respect to the angle θ are shown in Fig. 10 and the radial forces with the constant k are shown in Fig. 11. The lines show the linearity between the input k and the output forces. From Fig. 11, it can be seen that the radial force and the coefficient k have a proportional relationship. These results verify that k and

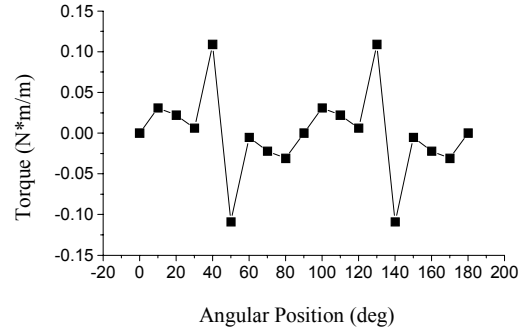


Fig. 9. Generated torque when control current arrangement for vertical force is applied

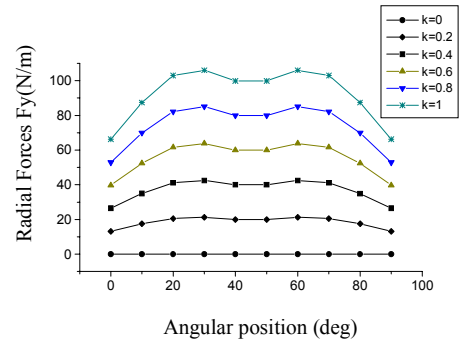


Fig. 10. Radial forces of various constant k with angle θ

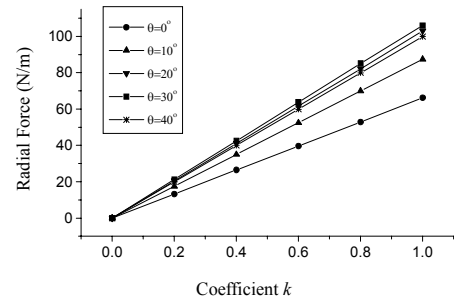


Fig. 11. Relationship between radial forces and constant k

forces vary with linear relationship, a linear feedback control method can be adopted for levitation control.

IV. EXPERIMENTAL RESULTS

Based on the above analyses, a prototype of the bearingless motor with rectifier circuit coil has been fabricated. The A-phase stator exciting winding configuration is shown in Fig. 12. The exciting winding

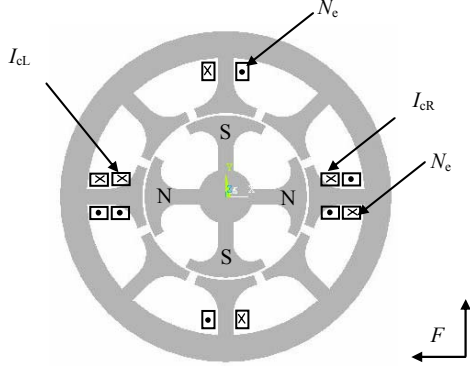


Fig. 12. A-phase exciting winding configuration

N_e consists of four coils connected in series. The horizontal radial forces with respect to control currents have been measured when the exciting voltage is 8V, 16V and 0 V respectively, and the AC voltage frequency is 800Hz. Fig. 13 shows the generated radial forces when only the control current I_{cL} is applied. It can be seen that when the exciting voltage is zero, the direction of the radial force does not change with the control current. However, when the exciting voltage showed in Fig. 12 is applied to the exciting winding, the negative force is produced as the control current I_{cL} changes its direction. It indicates that the existence of rectified coil makes the rotor possess a fixed polarity and have the characteristic of a permanent magnet.

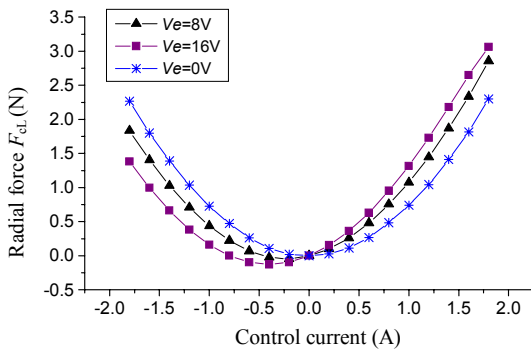


Fig. 13. Radial force when just control current I_{cL} is applied

The radial forces have also been measured when only the control current I_{cR} is applied, and the results are shown in Fig. 14.

When the control currents I_{cL} and I_{cR} are applied to the control current coils at the same time, the measured radial forces are shown in Fig. 15. It can be seen that these values are rightly equal to the summation of F_{cL} and F_{cR} .

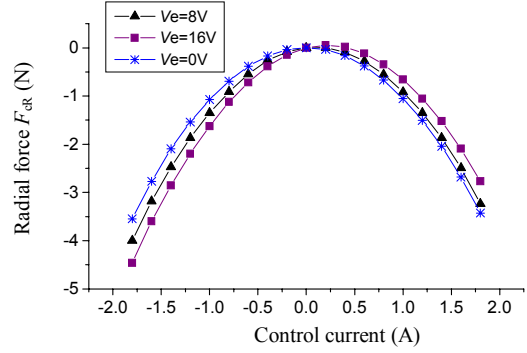


Fig. 14. Radial force when just control current I_{cR} is applied

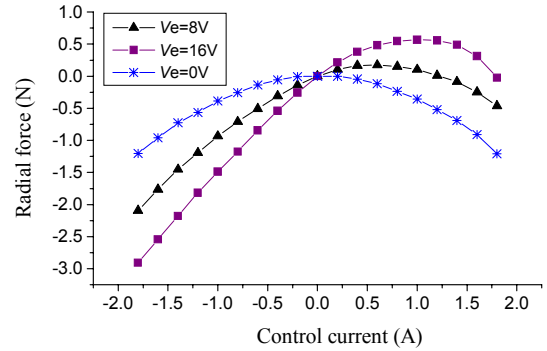


Fig. 15. Radial forces when both I_{cL} and I_{cR} are applied

V. CONCLUSIONS

For making the new type of bearingless motor, the design of the motor has been proposed and the feasibility of the designed motor has been checked by FEM analyses. By the analyses of the generated torques, it is verified that the sufficient torque can be obtained and the most appropriate tooth length has been determined. By the analyses of the produced radial forces, it is also verified that the sufficient forces can be obtained. And for feedback control, linearity of the input currents and the output forces has been verified. These results indicate that the proposed bearingless motor with rectifier circuits can be realized.

REFERENCES

- [1] K. Ohmori, S. J. Kim, T. Masuzawa and Y. Okada, "Design of an axial type self-bearing motor for small axial pump," Proc. of the Eighth international symposium on magnetic bearings, pp. 15-20, August 2002.
- [2] A. Chiba, Desmond T. Power, and M. Azizur Rahman, "Analysis of no-load characteristics of a bearingless induction motor," IEEE Transactions on industry applications, vol. 31, No.1, pp.77-83, January/February 1995.
- [3] Andres O. Salazar, A. Chiba and T. Fukao, "A review of developments in bearingless motors," 7th international symp. on magnetic bearings, pp.335-340, August, 2000.
- [4] Koichi Oka, "Bearingless motor with rectifier circuits," 8th international symposium on magnetic bearing, Mito, Japan pp.271-275, August, 2002.